Coupled antiferromagnetic spin-$\frac{1}{2}$ chains in green dioptase $Cu_6[Si_6O_{18}] \cdot 6H_2O$

A. Podlesnyak,[1,*] L. M. Anovitz,[2] A. I. Kolesnikov,[3] M. Matsuda,[1] T. R. Prisk,[2] S. Toth,[4] and G. Ehlers[1]

[1]*Quantum Condensed Matter Division, Oak Ridge National Laboratory, Oak Ridge, Tennessee 37831, USA*

[2]*Chemical Sciences Division, Oak Ridge National Laboratory, Oak Ridge, Tennessee 37831, USA*

[3]*Chemical and Engineering Materials Division, Oak Ridge National Laboratory, Oak Ridge, Tennessee 37831, USA*

[4]*Laboratory for Neutron Scattering and Imaging, Paul Scherrer Institut, CH-5232 Villigen PSI, Switzerland*

(Received 24 September 2015; published 23 February 2016)

In this paper, we report inelastic neutron scattering measurements of the magnetic excitations of green dioptase $Cu_6[Si_6O_{18}] \cdot 6H_2O$. The observed spectrum contains two magnetic modes and a prominent spin gap that is consistent with the ordered ground state of Cu moments coupled antiferromagnetically in spiral chains along the c axis and ferromagnetically in ab planes on the hexagonal cell. The data are in excellent agreement with a spin-$\frac{1}{2}$ Hamiltonian that includes antiferromagnetic nearest-neighbor intrachain coupling $J_c = 10.6(1)$ meV, ferromagnetic interchain coupling $J_{ab} = -1.2(1)$ meV, and exchange anisotropy $\Delta J_c = 0.14(1)$ meV. We calculated the sublattice magnetization to be strongly reduced, $\sim 0.39\mu_B$. This appears compatible with a reduced Néel temperature, $T_N = 14.5\ \mathrm{K} \ll J_c$, and can be explained by a presence of quantum spin fluctuations.

DOI: 10.1103/PhysRevB.93.064426

I. INTRODUCTION

Gem crystals of natural dioptase with colors ranging from emerald green to bluish have delighted people since ancient times and still attract the attention of mineral collectors around the globe. The first scientific investigations of dioptase date to the 19th century when its formal chemical composition was established as $Cu_6[Si_6O_{18}] \cdot 6H_2O$ [1]. Depending on the dehydration level, three varieties of dioptase, namely, natural green and blue $Cu_6[Si_6O_{18}] \cdot 6H_2O$, and black phase $Cu_6Si_6O_{18}$, are distinguished [2]. The crystal structure of green dioptase (space group $R\bar{3}$) consists of corrugated silicate rings of Si_6O_{18} interconnected by Cu^{2+} ions. Analogous rings of water molecules $6H_2O$ alternate with the silicate rings along the c axis [3,4]. Oxygen atoms form an axially elongated octahedral of $CuO_4(H_2O)_2$. The early studies of dioptase were limited to measurements of the structural and chemical properties until the first evidence for a magnetic ground state was obtained from NMR and heat capacity measurements [5,6]. Detailed investigations of its magnetic susceptibility, specific heat, and neutron diffraction proved the presence of long-range antiferromagnetic (AFM) ordering at a Néel temperature $T_N \sim 14.5$ K and a reduced Cu ordered magnetic moment $\sim 0.5\mu_B$ [7–9].

The magnetic ground state of green dioptase remains controversial. Each Cu^{2+} ion has two Cu nearest neighbors (NN) in a helical chain along the c axis and only one Cu in-plane neighbor forming a threefold spin-$\frac{1}{2}$ network. Two exchange interactions thus have major importance and determine the magnetic structure, namely, NN intrachain coupling J_c along the spiral chain and NN interchain coupling J_{ab} which forms Cu dimers in the ab plane (Fig. 1) [10,11]. Depending on the J_{ab}/J_c ratio, different kinds of the magnetic ordering can be expected, going from one-dimensional (1D) helical chainlike ordering for $|J_c| \gg |J_{ab}|$ to magnetic dimer formation in the case of $|J_c| \ll |J_{ab}|$. Both extreme cases would lack long-range magnetic order.

Both exchange interactions, J_c and J_{ab}, can be either negative or positive, which suggests a rich magnetic phase diagram. From the neutron diffraction and magnetic susceptibility of black (dehydrated) dioptase, Wintenberger *et al.* proposed that (a) intrachain exchange interactions are AFM, $J_c > 0$, and interchain ones are ferromagnetic (FM), $J_{ab} < 0$, and (b) $|J_{ab}|$ is substantially lower than $|J_c|$ [7]. These conclusions were supported by extended Hückel tight-binding calculations which found that black dioptase is an $S = \frac{1}{2}$ uniform AFM chain system in which the interchain spin exchange is weaker than the intrachain exchange by two orders of magnitude [12]. On the other hand, Gros and co-workers proposed that for fully hydrated green dioptase both J_c and J_{ab} are positive, corresponding to AFM coupling within and between the chains [10]. Their quantum Monte Carlo calculations predict that the system is close to a quantum critical point (QCP) between an AFM ordered state ($J_{ab}/J_c < 1.86$) and a quantum spin liquid ($J_{ab}/J_c > 1.86$). In contrast, Janson *et al.* claimed that $J_c > 0$ and $J_{ab} < 0$ for green dioptase [11]. Based on full-potential density functional theory calculations, they suggested the values of the coupling constants are $J_c = 6.72$ meV and $J_{ab} = -3.19$ meV with $J_{ab}/J_c \sim -0.5$.

In light of this controversy, we studied the magnetic interactions in green dioptase $Cu_6[Si_6O_{18}] \cdot 6H_2O$ using inelastic neutron scattering. By analyzing the features of the magnetic excitations, and fitting them with spin-wave calculations of a model spin Hamiltonian, we unambiguously determined the strength of the interactions and the magnetic order of green dioptase.

II. EXPERIMENT

Natural single crystals of green dioptase were obtained for these experiments. The material run on the time-of-flight Cold Neutron Chopper Spectrometer (CNCS) was originally from the Tsumeb Mine in Namibia (provided courtesy of the American Museum of Natural History, New York) and

*Corresponding author: podlesnyakaa@ornl.gov

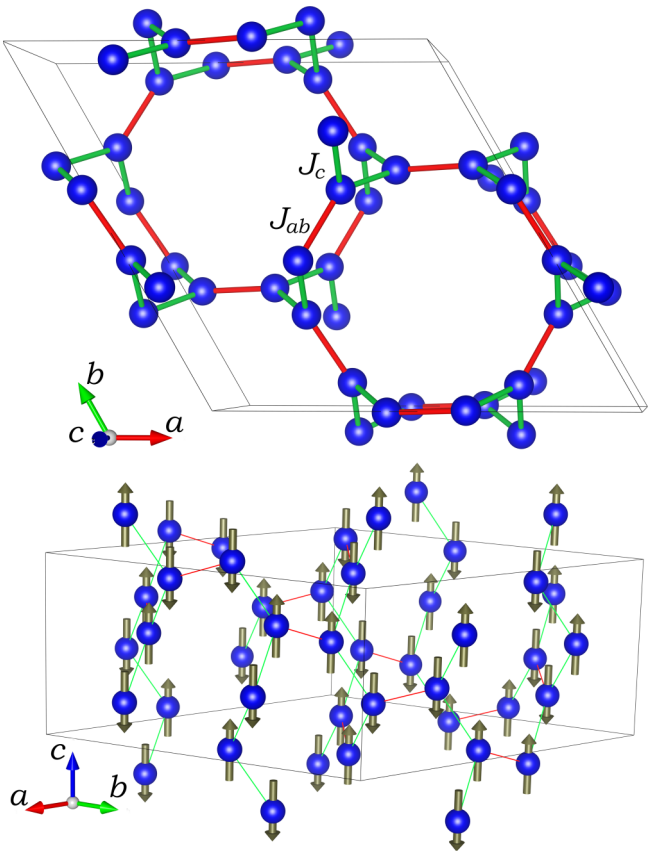

FIG. 1. Simplified crystal (top) and magnetic (bottom) structure of green dioptase showing $S = \frac{1}{2}$ Cu atoms only. Both magnetic exchange interactions, along the spiral chain J_c (green) and interchain J_{ab} (red), are indicated.

Reneville, Brazzaville Department, Republic of Congo. These were cut into 32 thin slabs $\sim\frac{3}{4}$ mm thick parallel to the c axis. The total sample mass was 4.4 g. The sample used for the experiments on the HB-1 triple axis spectrometer was also a natural single crystal originally obtained from the Okawandasi Mine, Kunene Region, Namibia, weighing approximately 1 g, 22 mm along the c axis and 4 mm across the diameter. This sample was oriented and run uncut. The latter two samples were obtained commercially.

Inelastic neutron scattering measurements were performed using the CNCS [13] at the Spallation Neutron Source at Oak Ridge National Laboratory. The sample was mounted in the $(H0L)$ scattering geometry in an "orange" continuous flow liquid He cryostat. Note that here and elsewhere in this paper we use the hexagonal setting. The measurements were carried out using a rotating single crystal method at temperatures of $T = 1.7$, 6.0, and 25 K. The detector coverage out of plane was about $\pm 15^\circ$, so that a limited Q range along the K direction could also be accessed. The data were collected using fixed incident neutron energies of 12.0 and 3.1 meV, which allowed the measurement of excitations up to energy transfers of $\hbar\omega \sim 11.0$ meV and ~ 2.8 meV, respectively. In these configurations, a full width at half maximum resolution of 0.38 and 0.07 meV was obtained at the elastic position. The crystal mosaicity was found to be about 3° and thus accounts for the dominating contribution to the Q resolution over the measured range of reciprocal space. The excitation spectra were recorded while rotating the sample in a 100° range with 2° steps. For the simulated cuts we convoluted the spin-wave spectrum with the finite mosaicity, bin window, and instrumental energy resolution. The detector efficiency correction was performed using a vanadium reference sample. To unambiguously define the energy scale of the magnetic excitations, additional inelastic neutron scattering measurements along selected high-symmetry directions were performed at temperatures of $T = 4$ and 20 K using the HB-1 triple axis spectrometer at the HFIR reactor at Oak Ridge National Laboratory. The measurements were carried out using pyrolitic graphite crystals for the monochromator and analyzer, operating at a fixed final energy of 13.5 meV. The collimation was set at 48′-80′-80′-120′, producing an energy resolution of 1.5 meV at the elastic position. To reduce higher-order wavelength contamination, a pyrolitic graphite filter was placed after the sample. The MANTIDPLOT [14], HORACE [15], and DAVE [16] software packages were used for data reduction and analysis of the data sets. Linear spin-wave theory, as realized in the SPINW program package [17], was used to calculate the excitation spectra and neutron scattering cross section of the spin Hamiltonian.

III. RESULTS AND DISCUSSION

The scattering intensity as a function of Q and energy transfer along selected high-symmetry crystal orientations, obtained using the CNCS, are summarized in Fig. 2 (top

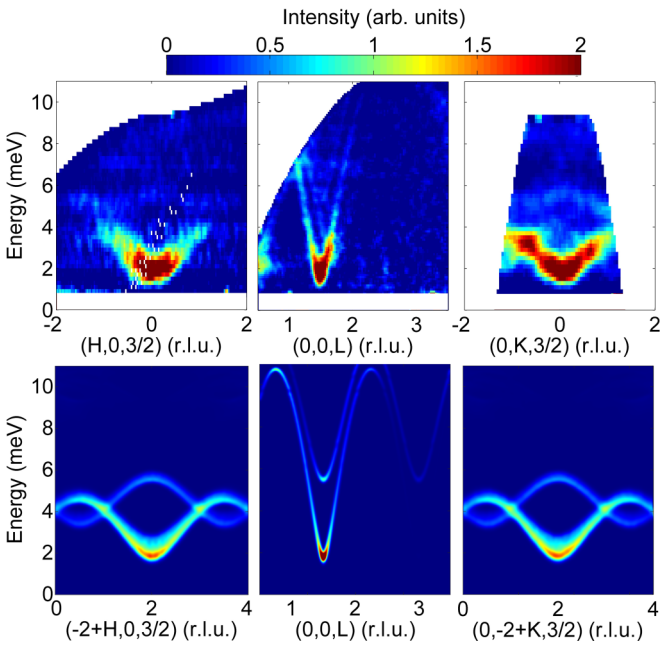

FIG. 2. The $\sigma(\mathbf{Q}, E)$ slices through the four-dimensional inelastic neutron data sets measured at CNCS in green dioptase at $T = 1.7$ K, showing the dispersion of magnetic excitations along high-symmetry directions. Top: Background-subtracted experimental data. The integration along the H, K, or L directions is ± 0.1 r.l.u. Bottom: Simulation, based on the model cross section and the fitted parameter values, and convoluted with the spectrometer resolution, as described in the text. Note that r.l.u. stands for reciprocal lattice units.

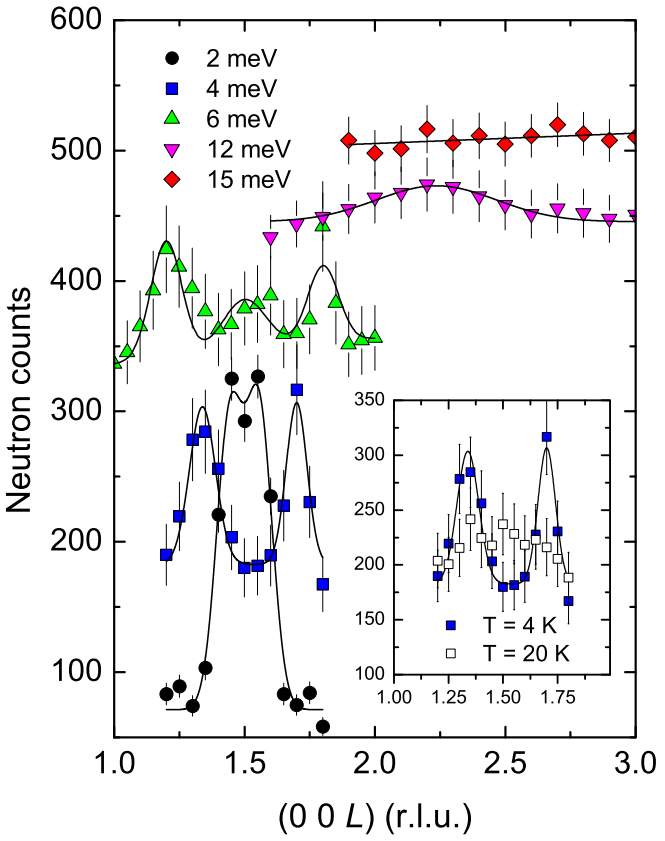

FIG. 3. Constant energy scans $\Delta\hbar\omega$ along the $(0\,0\,L)$ direction at several energy transfers as measured on the HB-1 triple axis spectrometer at $T = 4$ K. The lines are a guide to the eye. The baselines have been shifted for each energy transfer for clarity. The inset shows the $\Delta\hbar\omega = 4$ meV scan at $T = 4$ K (solid squares) and $T = 20$ K (open squares).

panel). To emphasize the magnetic scattering, the nonmagnetic background was subtracted. We simulated the background for a two-dimensional (2D) slice by using the signal at high **Q** in a 1D cut and then replicating it into 2D and subtracting from the real data. For the $(H03/2)$ data the H range was $1.8 < H < 2.0$ r.l.u.; for the $(00L)$ data the L range was $2.7 < L < 3.2$ r.l.u. For the out-of-plane direction $(0K3/2)$ we used $([1.8–2.0]0\frac{3}{2})$ data. The integration along other directions was ± 0.1 r.l.u. The observed spectrum comprises two distinct dispersive magnetic modes, suggesting that the excitations are spin waves and the magnetic structure has two sublattices. Both spin-wave modes are gapped—the minimum of the dispersion curves at the center of the Brillouin zone does not go to zero energy ($\Delta_{\min} \neq 0$). Instead, the spin excitation spectrum has an energy gap $\Delta_{\min}$ of $\sim$1.5 meV at $(00\frac{3}{2})$. The inelastic scattering is strongest around an (HKL) of (0 0 1.5), which is consistent with a propagation vector of $(00\frac{3}{2})$. The bandwidths of the magnetic excitations were found to be very different parallel and perpendicular to L. The larger bandwidth along L suggests that $J_c > J_{ab}$. Measurement of the spin excitation energies using the HB-1 triple-axis spectrometer along L shows that the tops of the spin-wave bands reach $\sim$12 meV (Fig. 3). Inelastic scans along the $(H0\frac{3}{2})$ and $(0K\frac{3}{2})$ directions show that the dispersion curves in the $(HK0)$ plane have a maximum energy of $\sim$5.5 meV. Comparison of HB-1 data at 4 and 20 K [Fig. 3 (inset)] shows that the spin waves are sharp and well defined below T_N, and broad and significantly damped above T_N. A similar result was obtained at 6 and 25 K on CNCS (not shown).

As outlined in the Introduction, several models for the magnetic ground state and exchange interactions in green dioptase have been proposed. Since the material exhibits long-range AFM ordering, the case when both J_{ab} and J_c are negative (FM) can be ruled out. The uniform AFM $S = \frac{1}{2}$ chain system [12] with $J_{ab} \sim 0$ and $J_c > 0$ proposed for the black dioptase $Cu_6Si_6O_{18}$ would result in a spinon spectrum along $(00L)$ and no dispersion in the $(HK0)$ plane. The energy scale is determined by the value of J_c. Another extreme case, $J_c \sim 0$, would lead to the formation of a $S = \frac{1}{2}$ dimer system. The spin Hamiltonian splits the electronic ground state into a singlet ($S = 0$) and a triplet ($S = 1$) with an energy separation equal to J_{ab} [18]. In the case of dimerization, the triplet modes could also be dispersive when considering further magnetic exchanges. However, a long-range magnetic ordering [9] with a sign of a first-order phase transition in the heat capacity [8], rules out dimerization. Both magnetic exchange interactions, J_c and J_{ab}, therefore have nonzero values.

We compare the inelastic neutron scattering cross section $\sigma(\mathbf{Q}, E)$ quantitatively with the spin-spin correlation function calculated from linear spin-wave theory and multiplying it with the squared magnetic form factor of Cu^{2+} ions. We propose the following minimum Hamiltonian to fit the experimental data:

$$\mathcal{H} = \sum_{\langle i,j\rangle_c} J_c \mathbf{S}_i \cdot \mathbf{S}_j + \Delta J_c S_i^z S_j^z + \sum_{\langle i,j\rangle_{ab}} J_{ab} \mathbf{S}_i \cdot \mathbf{S}_j, \quad (1)$$

where the summations run over $\langle i,j\rangle_c$ and $\langle i,j\rangle_{ab}$, which denote bonds along the chains and bonds in the ab plane, respectively. The observed spin-wave gap can be alternatively reproduced using an easy axis anisotropy on every Cu^{2+} ion by adding the following single ion anisotropy term to the Hamiltonian:

$$\mathcal{H}_A = -\sum_i A S_i^{z2}, \quad (2)$$

where S_i^z is the classical value of the spin [19]. The same gap can be reproduced if $A = \Delta J_c$. From linear spin-wave theory alone we cannot tell which model is correct. To fit the observed spin-wave dispersions, the experimental energies at several wave vectors were taken along all three high-symmetry directions. The standard least squares fitting procedure of the dispersion relations was used to get best fit. This yielded the following exchange parameters, in meV: $J_{ab} = -1.2(1)$, $J_c = 10.6(1)$, and $\Delta J_c = A = 0.14(1)$. In order to compare the above model results with the experimental data, the calculated spin-spin correlation function was convoluted with the instrumental resolution function [13]. The intensities of the calculated spin waves were scaled to agree with the experiment [Fig. 2 (bottom panel)]. Figure 4 shows a comparison of the measured and simulated intensity on the $(H0L)$ plane at different energies. The exchange parameters obtained perfectly reproduce both the shape of the spin-wave dispersion for each of the three high-symmetry directions

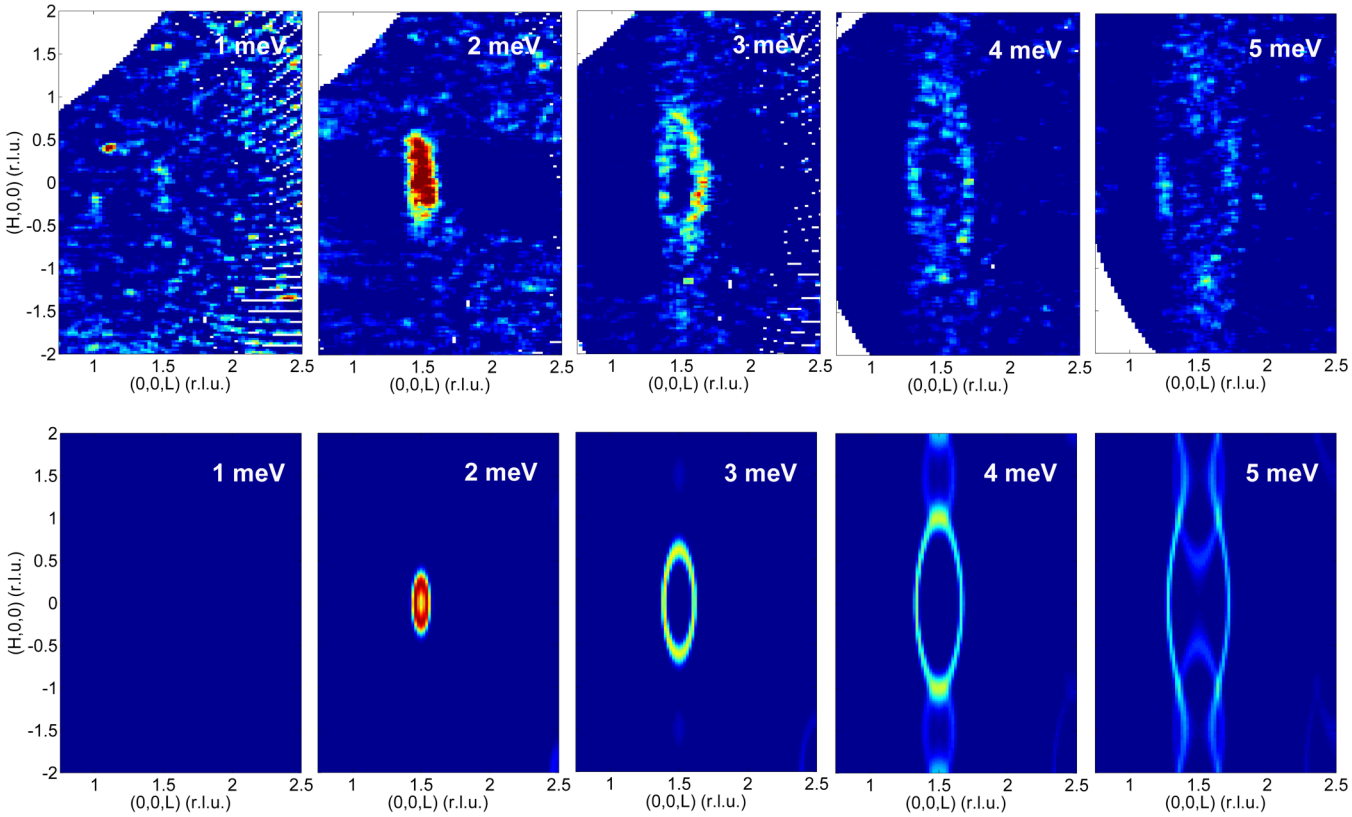

FIG. 4. Measured (top) and simulated (bottom) constant energy maps for the green dioptase at $T = 1.7$ K.

and their relative intensities. Note that the values obtained for J_{ab} and J_c are in a quantitative disagreement with the parameters published in Ref. [11] ($J_{ab} = -3.2$ meV and $J_c = 6.7$ meV), possibly because the fit in Ref. [11] was based on magnetization data only. The anisotropy term, assuming single ion anisotropy, is comparable to density functional theory (DFT) results on several Cu^{2+} compounds [19]. We expect that due to the small $S = \frac{1}{2}$ spin quantum number, corrections to linear spin-wave theory are necessary. The main correction is the renormalization of the spin-wave energies with a momentum independent constant Z that is often >1 ($Z_c = 1.18$ for square lattice antiferromagnets [20]). As a result, the real exchange constants can be smaller than our fitted values.

Linear spin-wave theory can also estimate the size of the sublattice magnetization. Calculated from our Hamiltonian, the size of the ordered moment is $0.38\mu_B$, in reasonable agreement with neutron diffraction data, $0.55(1)\mu_B$ [9]. The presence of quantum fluctuations due to the small Cu-Cu coordination number is a plausible explanation for this low value as well as for a reduced Néel temperature ($T_N \sim 14.5$ K) in comparison to $J_c \sim 123$ K.

IV. CONCLUSIONS

To summarize, a spin-wave model with two exchange interactions, an NN AFM intrachain coupling $J_c = 10.6(1)$ meV, NN FM interchain coupling $J_{ab} = -1.2(1)$ meV, and exchange or single ion anisotropy of $\Delta J_c = 0.14(1)$ meV, is shown to provide a good description of the observed magnetic excitations in green dioptase. Our study proves that the magnetic ground state features spiral AFM spin chains along the hexagonal c axis with FM interchain coupling, in agreement with Refs. [9,11], and it disagrees with the picture of green dioptase as an antiferromagnet close to a quantum critical point, as suggested by Ref. [10].

ACKNOWLEDGMENTS

Research at Oak Ridge National Laboratory's Spallation Neutron Source and High Flux Isotope Reactor was supported by the Scientific User Facilities Division, Office of Basic Energy Sciences, U.S. Department of Energy. This research was sponsored by the Division of Chemical Sciences, Geosciences, and Biosciences, Office of Basic Energy Sciences, U.S. Department of Energy. This manuscript has been authored by UT-Battelle, LLC under Contract No. DE-AC05-00OR22725 with the U.S. Department of Energy. The United States Government retains and the publisher, by accepting the article for publication, acknowledges that the United States Government retains a nonexclusive, paid-up, irrevocable, worldwide license to publish or reproduce the published form of this manuscript, or allow others to do so, for United States Government purposes. The Department of Energy will provide public access to these results of federally sponsored research in accordance with the DOE Public Access Plan (http://energy.gov/downloads/doe-public-access-plan).

[1] H. Hess, Chemishe analyse des dioptases, Ann. Phys. (Leipzig) **16**, 360 (1829).

[2] H. G. Heide, K. Boll-Dornberger, E. Thilo, and E. M. Thilo, Die struktur des dioptas, $Cu_6[Si_6O_{18}] \cdot 6H_2O$, Acta Crystallogr. **8**, 425 (1955).

[3] P. H. Ribbe, G. V. Gibbs, and M. M. Hamil, A refinement of the structure of dioptase, $Cu_6[Si_6O_{18}] \cdot 6H_2O$, Am. Mineral. **62**, 807 (1977).

[4] K.-H. Breuer, W. Eysel, and R. Müller, Structural and chemical varieties of dioptase, $Cu_6[Si_6O_{18}] \cdot 6H_2O$, Z. Kristallogr. **187**, 15 (1989).

[5] R. D. Spence and J. H. Muller, Proton resonance in dioptase $(CuSiO_3 \cdot H_2O)_6$, J. Chem. Phys. **29**, 961 (1958).

[6] W. R. Eisenberg and H. Forstat, Further evidence for a magnetic transition in dioptase, J. Phys. Soc. Jpn. **19**, 406 (1964).

[7] M. Wintenberger, G. André, and M. F. Gardette, Magnetic properties of green dioptase $CuSiO_3 \cdot H_2O$ and of black dioptase $CuSiO_3$ and magnetic structure of black dioptase, Solid State Commun. **87**, 309 (1993).

[8] I. A. Kiseleva, L. P. Ogorodova, L. V. Melchakova, and M. R. Bisengalieva, Thermodynamic properties of copper silicate: dioptase: $Cu_6[Si_6O_{18}] \cdot 6H_2O$, J. Chem. Thermodyn. **25**, 621 (1993).

[9] E. L. Belokoneva, Y. K. Gubina, J. B. Forsyth, and P. J. Brown, The charge-density distribution, its multipole refinement and the antiferromagnetic structure of dioptase, $Cu_6[Si_6O_{18}] \cdot 6H_2O$, Phys. Chem. Miner. **29**, 430 (2002).

[10] C. Gros, P. Lemmens, K.-Y. Choi, G. Güntherodt, M. Baenitz, and H. H. Otto, Quantum phase transition in the dioptase magnetic lattice, Europhys. Lett. **60**, 276 (2002).

[11] O. Janson, A. A. Tsirlin, M. Schmitt, and H. Rosner, Large quantum fluctuations in the strongly coupled spin-$\frac{1}{2}$ chains of green dioptase $Cu_6[Si_6O_{18}] \cdot 6H_2O$, Phys. Rev. B **82**, 014424 (2010).

[12] J. M. Law, C. Hoch, M.-H. Whangbo, and R. K. Kremer, Description of anhydrous (black) dioptase as a $S = 1/2$ uniform antiferromagnetic chain system, Z. Anorg. Allg. Chem. **636**, 54 (2010).

[13] G. Ehlers, A. Podlesnyak, J. L. Niedziela, E. B. Iverson, and P. E. Sokol, The new cold neutron chopper spectrometer at the Spallation Neutron Source: Design and performance, Rev. Sci. Instrum. **82**, 085108 (2011).

[14] O. Arnold, J. C. Bilheux, J. M. Borreguero, A. Buts, S. I. Campbell, L. Chapon, M. Doucet, N. Draper, R. Ferraz Leal, M. A. Gigg, V. E. Lynch, A. Markvardsen, D. J. Mikkelson, R. L. Mikkelson, R. Miller, K. Palmen, P. Parker, G. Passos, T. G. Perring, P. F. Peterson, S. Ren, M. A. Reuter, A. T. Savici, J. W. Taylor, R. J. Taylor, R. Tolchenov, W. Zhou, and J. Zikovsky, MANTID - data analysis and visualization package for neutron scattering and μSR experiments, Nucl. Instrum. Methods Phys. Res., Sect. A **764**, 156 (2014).

[15] Available at http://horace.isis.rl.ac.uk

[16] R. Azuah, L. Kneller, Y. Qiu, P. Tregenna-Piggott, C. Brown, J. Copley, and R. Dimeo, DAVE: A comprehensive software suite for the reduction, visualization, and analysis of low energy neutron spectroscopic data, J. Res. Natl. Inst. Stand. Technol. **114**, 341 (2009).

[17] S. Toth and B. Lake, Linear spin wave theory for single-Q incommensurate magnetic structures, J. Phys.: Condens. Matter **27**, 166002 (2015).

[18] A. Furrer and H. U. Güdel, Neutron inelastic scattering from isolated cluster of magnetic ions, J. Magn. Magn. Mater. **14**, 256 (1979).

[19] J. Liu, H.-J. Koo, H. Xiang, R. K. Kremer, and M.-H. Whangbo, Most spin-1/2 transition-metal ions do have single ion anisotropy, J. Chem. Phys. **141**, 124113 (2014).

[20] R. R. P. Singh, Thermodynamic parameters of the $T = 0$, spin-1/2 square-lattice Heisenberg antiferromagnet, Phys. Rev. B **39**, 9760 (1989).